Propagation Loss for Trans-Horizon Interferences in the Regions Surrounding Deep Space Network Complexes

C. Ho,[1] K. Angkasa,[2] P. Kinman,[3] and T. Peng[4]

With potential future deployment of high-density terrestrial communication systems in metropolitan areas, it becomes necessary to estimate potential interference received at the Deep Space Network (DSN) Earth station from interfering sources distributed in the region. A fundamental parameter required for any realistic interference analysis is the propagation loss from the transmitter to the receiver, which depends in a statistical way on the atmospheric conditions. This article introduces a method of constructing a map of propagation losses covering almost every possible location in the region, taking the terrain into account. The losses were computed with a high-resolution terrain map of the region as input, together with the heights of the transmitting and receiving antennas. The calculation includes three clear-air propagation mechanisms: diffraction, tropospheric scattering, and atmospheric ducting, in accordance with the algorithms given in the International Telecommunication Union Recommendation ITU-R P.452. The resulting numerical database provides propagation-loss data necessary for interference calculations. To enhance visualization, these propagation-loss data are mapped in color. The color-coded propagation loss map provides a visible overview of the entire region of interest, indicating areas where emissions from the terrestrial sources would be effectively shielded by the terrain from reaching the DSN Earth stations, and where such emissions should be restricted for lack of terrain shielding.

I. Introduction

The Earth stations in the Deep Space Communication Complexes (DSCCs) are increasingly threatened by potential growth of microwave interference sources in the surrounding urban areas. Mobile phones are used everywhere [1,2]. Fixed terminals are starting to be widely used in commercial centers in metropolitan areas [3]. With growing demand for high-volume communications, these commercial services also are moving to higher-frequency bands. Some of these bands are also allocated to space research. For

[1] Communications Architectures and Research Section.

[2] Communications Ground Systems Section.

[3] Case Western Reserve University, Cleveland, Ohio.

[4] DSMS Commitments Office.

The research described in this publication was carried out by the Jet Propulsion Laboratory, California Institute of Technology, under a contract with the National Aeronautics and Space Administration.

example, the 31.8- to 32.3-GHz and 37- to 38-GHz bands have been allocated in the Radio Regulations of the International Telecommunication Union (ITU) to both the Space Research Service and the terrestrial Fixed Service [3]. (Within the United States of America (USA), the 31.8- to 32.3-GHz band is not allocated to the Fixed Service.) All of these deployments have potential interference scenarios with DSCCs.

The Earth stations in the DSCCs use large-aperture antennas and sensitive receivers to receive very weak signals from spacecraft at planetary distances [4]. It is crucial that these receivers not be affected by interferences beyond an acceptable limit. The ITU has established protection criteria for the Space Research Service in terms of a threshold level of received power which should not be exceeded except for a specified small percent of time as defined in Recommendations ITU-R 1157 [5] and 1396 [6].

These protection criteria do not allow any interference from sources in the line of sight. The numerical criteria thus apply specifically to interferences arriving from the other side of the physical horizon, or trans-horizon, through the atmosphere [7]. The instantaneous level of such interference depends on atmospheric conditions [8]. Consequently, the propagation loss through the atmosphere is modeled statistically, based on measurement [9]. The ITU has conducted extensive measurement of trans-horizon propagation over many years. The results are presented as statistical propagation-loss models in Recommendation ITU-R P.452 [10]. Parameter values of water-vapor density used in this study also are according to the recommendation. This study addresses trans-horizon interference by applying three clear-air propagation mechanisms: diffraction, tropospheric scattering, and atmospheric ducting/layer reflection. For the diffraction mechanism, additional data from Recommendation ITU-R P.526 are also used [11]. This study has not included consideration of clutter losses due to buildings and vegetation. Nor has it included propagation losses in hydrometeor scattering.

Recommendation P.452 characterizes the propagation loss from a specific transmitter location to a specific receiver location [10]. We have extended the calculation to characterize the propagation losses from almost all possible mapped transmitter locations surrounding the receiver location. As examples, the method is applied to the Deep Space Communication Complexes at Goldstone, California, USA; at Tidbinbilla near Canberra, Australia; and at Robledo near Madrid, Spain.

Section II describes the technical approach. Section III describes contents of the terrain profile needed for propagation-loss calculation. Section IV describes the propagation-loss algorithms and assumptions for calculations. Section V presents examples of applying this method to the three DSCCs. Section VI presents the conclusion.

II. Technical Approach

The technical approach is chosen to address the area-to-point interference problem mentioned above. The trans-horizon propagation loss from a transmitter to the Earth station receiver can be calculated in accordance with Recommendation ITU-R P.452 [10]. A set of sample locations is selected to cover the area surrounding the Earth station with a resolution comparable to the resolution of available terrain data. Propagation losses first are calculated for the sample locations along a radial direction from the Earth station. The calculation then is repeated along 360 directions in steps of 1 deg, corresponding to 360 deg of azimuth angle. The result is the propagation-loss estimates at these sample points covering the entire area of interest. When plotted on a two-dimensional map, the result provides visualization of the dependence of propagation loss on terrain, radial distance, and azimuth angle from the Earth station.

A. Propagation Loss Between Any Two Points

For an accurate estimate of the propagation loss between a transmitter and the receiver, it is necessary to account for the locations and heights of the transmitter and the receiver and the effects of the terrain and atmosphere in between.

The terrain data file must have sufficient horizontal resolution to capture the hilltops in the immediate vicinity of the Earth station. These local hilltops define the physical horizons around the Earth station. The elevation angle of the physical horizon as seen by the Earth-station antenna in an azimuth direction determines to a large extent the propagation loss along that direction. To capture adjacent hilltops around the three Deep Space Communication Complexes, the terrain maps need to have a horizontal grid of 100 m or finer in order to achieve acceptable accuracy of propagation-loss calculation.

Empirical models of propagation loss, including the effect of the atmosphere, are given in ITU-R P.452 for propagation along a great-circle path [10]. Those empirical models are given in the form of a cumulative distribution function. Given an Earth-station protection criterion, such as −220 dB (W/Hz), not to be exceeded more than 0.001 percent of the time in the 37- to 38-GHz band in order not to interfere with manned-space exploration (ITU-R SA.1396) [6], one can estimate the propagation loss at the lowest 0.001 percentile. With the propagation loss estimated at the lowest 0.001 percentile, the interference power is at the highest 0.001 percentile. This value then can be compared with the protection criterion.

For clear-air propagation, propagation-loss models include line of sight, diffraction, tropospheric scattering and ducting, and layer reflection [10]. The Deep Space Network (DSN) Earth stations are surrounded by hills in the immediate vicinity of the Earth stations. Terrestrial transmitters are expected only on the other side of the hills, with no line of sight from the Earth stations.

B. From Transmitter Locations Along a Radial Direction

The propagation loss first is calculated for a set of uniformly spaced locations along a single radial direction from the Earth station. This computation is sufficient because all locations along the same radial direction share the same terrain profile.

C. From Transmitter Locations in All Directions

Such calculations are repeated for 359 other radial directions, spaced 1 deg apart. Enough data then exist to show how the propagation loss varies throughout the area surrounding the Earth station.

III. Terrain Profile

The location of each of the three Deep Space Stations (DSSs) is represented by the geodetic coordinates of the 70-m antenna in the complex, as given in Table 1. The terrain map around each complex is obtained from the Institute for Telecommunication Sciences, National Telecommunications and Information Administration. Each map consists of terrain elevation with 1-m precision at locations separated horizontally by 100 m. Data on the terrain map are arranged in 360 terrain profiles, one for each azimuth angle. Each profile contains data for locations at every 100-m interval along a radial direction emanating from the 70-m antenna.

Propagation-loss models [10] are given in terms of geometrical quantities defined in the great-circle plane containing the path from the transmitter to the receiver and the terrain profile in between. These quantities, including the concept of angular distance, are summarized and explained in the Appendix.

Table 1. Coordinates of three DSN stations with a 70-m antenna.

Station name	Location	Latitude	Longitude	Elevation, m
DSS 14	Goldstone, USA	35.426 deg N	116.890 deg W	1002.1
DSS 43	Canberra, Australia	35.402 deg S	148.981 deg E	689.6
DSS 63	Robledo, Spain	40.431 deg N	4.248 deg W	865.5

The terrain profile needs to be modified to take into account the downward bending of a ray path in the atmosphere, where gases decrease in density with altitude. The degree of bending depends on the refractive index gradient existing in the atmosphere near the surface of the Earth. Recommendation ITU-R P.452 provides a method to account for the effect of ray-path bending on trans-horizon propagation over the terrain [10]. The method takes into account the effect of the Earth's atmosphere but with a larger Earth radius. This radius, called the effective Earth radius, is calculated to effectively bend the terrain profile upward such that the relative geometry between the modified terrain profile and a straight, unbent ray path would remain the same as before. The specific equations and parameters are summarized in the Appendix of this article.

IV. Propagation-Loss Calculations

The propagation loss of interest in this article is called the basic transmission loss and denoted $L_b(p)$ [10]. It is related to the transmitted power P_t, the transmit antenna gain (in the direction toward the receiver) G_t, the receive antenna gain (in the direction of the transmitter) G_r, and the received power $P_r(p)$ through the equation [7,10]

$$L_b(p) = P_t + G_t + G_r - P_r(p) \ \text{dB} \tag{1}$$

Defined in this way, the propagation loss is a positive number in decibels. Because the atmospheric conditions that determine the propagation loss are subject to change randomly, both the propagation loss $L_b(p)$ and the received power $P_r(p)$ are statistical in nature. In order to emphasize this, both of these quantities are shown as explicit functions of p, a time percentage. To be precise, $L_b(p)$ is the basic transmission loss not exceeded p percent of the time.

The function $L_b(p)$, which is modeled in Recommendation ITU-R P.452 [10], conveys the same information as a cumulative distribution function, and it is loosely referred to as such in this article. (Mathematically speaking, the true cumulative distribution function is the inverse function of $L_b(p)$ with p treated as a probability, rather than a percentage.)

In the case where a transmitter has a short, line-of-sight view of the receiver, the basic transmission loss is approximately deterministic and a function of only the range and wavelength. That is not the case of interest in this article. In general, propagation occurs along a trans-horizon path through the atmosphere, and the propagation loss depends on geometric parameters related to the terrain profile (for example, the horizon elevation angles as seen from the transmitter and receiver) and also on the physical parameters of the atmosphere (such as water-vapor density).

Since the DSN Earth stations are located in valleys surrounded by hills, there is practically no line of sight connecting these Earth stations and the terrestrial sources on the other sides of the hills. Interference from these terrestrial sources can reach the DSN Earth stations only by trans-horizon propagation mechanisms. Recommendation ITU-R P.452 has characterized the propagation losses in the clear-air and the rain-scattering (or hydrometeor scattering) propagation modes [10]. The trans-horizon clear-air mode includes three trans-horizon propagation mechanisms: diffraction, tropospheric scattering, and ducting/layer reflection. The mathematical models of these three mechanisms were used in this study to estimate trans-horizon propagation losses in clear air. These models are summarized in the Appendix of this article. The rain-scattering propagation-loss model is considerably more complicated than the clear-air models. While one can use this model to predict interference between two points, it is hard to combine terrain shielding effects with rain-scattering trans-horizontally and to draw general conclusions on transmitting sources distributed in an area. Therefore, we have not included rain-scattering propagation in this study, recognizing that such exclusion could in principle overestimate the propagation loss and underestimate total interference.

The following is a brief description of the geometric and physical parameters that have been taken into account in the propagation-loss models given in the Appendix of this article.

A. Loss in Diffraction [11]

Radio signals can be diffracted by hilltops or rounded obstacles and propagate beyond the line of sight. The loss in propagation by the diffraction mechanism depends on frequency, great-circle path distance, multi-path effects, and gas absorption as a function of water-vapor density. It also includes an effect of hilltops called the "knife edge effect." This effect depends on the heights of the hilltops relative to the heights of the transmitters and receivers and the horizontal distances of these terrain points, taking into account the effective Earth radius related to ray-path bending in the atmosphere. The propagation loss is given as a statistical distribution, indicating the percentage of time actual loss is below this value. The diffraction loss is calculated from Eq. (A-10) in the Appendix of this article, with parameter definitions given in Section II.

B. Loss in Tropospheric Scattering [10]

Radio signals can be scattered by particles and turbulence in the troposphere. Loss by this propagation mechanism is a function of frequency, great-circle path distance, angular distance between transmitter and receiver, aperture–medium coupling, surface refractivity, and gaseous absorption depending on water-vapor density. The loss also is presented as a function of the percentage of time the actual loss is below the calculated value; thus, it is a statistical distribution. The loss is calculated from Eq. (A-20), given in the Appendix, with parameter definitions and other specifics given in Section III.

C. Loss in Ducting/Layer Reflection [10]

Due to surface heating and radiative cooling, inversion temperature layers sometimes are generated on the ocean or flat coastal surface without large mountains. Radio signals can be trapped within this reflection layer at heights up to a few hundred meters and propagate over a long distance.

D. Comparison and Combination of Losses

The calculated propagation losses of these three mechanisms in a typical radial direction from Goldstone are given in Fig. 1. For the particular radial direction of Fig. 1 and within about 20 km of the Earth station, diffraction has the lowest propagation loss. At larger distances, tropospheric scattering has the lowest propagation loss, and the ducting and layer reflection mechanism has the highest propagation loss. Also shown in Fig. 1 is the combined effect (marked as "combined loss") of the three propagation losses, calculated by Eq. (A-47) of the Appendix, which originates from Recommendation ITU-R P.452, Table 5 [10].

V. Examples

This section provides examples of propagation-loss maps for possible use in the interference analysis between area-wide distributed terrestrial transmitters and the space research Earth stations in the 31.8- to 32-GHz and 37- to 38-GHz bands. The examples presented here include regions around the DSN complexes at Goldstone, Tidbinbilla, and Robledo.

At locations between the Earth station and its physical horizons, propagation losses are calculated as line-of-sight. At locations outside the physical horizons, the losses are calculated according to the combined effect, or overall prediction, of three trans-horizon mechanisms: diffraction, tropospheric scattering, and ducting and layer reflection, as given in Eq. (A-47) in the Appendix.

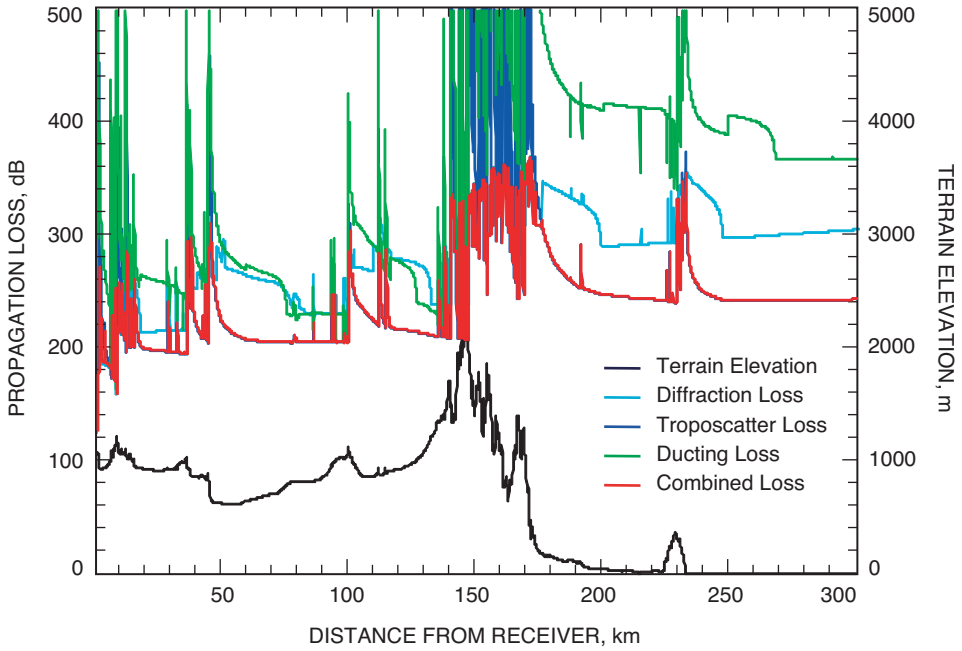

Fig. 1. Propagation losses and terrain profile in a radial direction at 217-deg azimuth angle from Goldstone. Losses are calculated at 32 GHz, exceeded all but 0.001 percent of the time. The aggregate of the three losses is marked in red, which most of the time is dominated by the minimum of the three types of propagation losses.

In each example, the terrain map provides elevation data at horizontal intervals of 100 m in 360 azimuth directions from the 70-m receive antenna, covering an area of 300-km radius. The transmit and receive antennas are assumed to have an antenna center height of 15 m and 37 m, respectively, measured from the local terrain level. The calculation of propagation loss is made from a transmit antenna to the receive antenna. The frequency is 32 GHz.

Three figures are presented for each example, identified with the letters (a), (b), and (c) in each case. Figure (a) presents the propagation losses from locations along one radial direction. Figure (b) presents the propagation losses from locations distributed over the two-dimensional map. Figure (c) presents the horizon elevation angles as a function of azimuth angle. The propagation losses represent values exceeded all but 0.001 percent of the time.

The loss calculations from which figure (a) was compiled used only a single terrain profile along a radial direction. The loss calculations from which figure (b) was compiled used a large set of terrain profiles, uniformly spaced in azimuth with an angular separation of 1 deg. Each terrain profile consists of a list of paired numbers, each number pair representing a physical point on the terrain. Each number pair consists of a distance from the receiver and a height above sea level with 1-m precision. The horizontal resolution of the terrain map is 100 m per physical point. The calculation of propagation loss is made exactly at these physical points.

For each point in figures (a) and (b), a propagation loss was calculated assuming that the transmitter was located at this point and the receive antenna was located at the 70-m antenna site. The loss values on the visible map given in the second figure are color-coded with a 5-dB resolution. Areas with low loss are shown in blue, and areas with high loss are shown in red. The middle colors of the rainbow are used to indicate medium losses. In general, blue indicates areas with low propagation losses, so consequently high interference powers from these areas are expected. These areas occur in the vicinities of all three

complexes. Attention should be paid to the transmission from such areas. As we proceed away from the deep-space antenna sites, the losses increase, especially in the areas shielded by mountains.

Two important parameters in the loss calculations are the horizon elevation angles as seen from the electrical centers of the transmit antenna and the receive antenna. The horizon elevation angles of the transmitter and the receiver were calculated using the terrain profile. The horizon elevation angle of the 70-m Earth station antenna is shown in the third figure as a function of azimuth angle.

The examples use the 70-m antenna site as the geometric center of calculations, the reference point for the terrain profiles and propagation-loss calculations. The same terrain database can be rearranged to center at another antenna site in the same DSN complex.

Example 1: Goldstone, California, USA. Figure 2(a) presents the effective propagation-loss values calculated along a radial direction at an azimuth angle of 217 deg from the 70-m antenna site (DSS 14) at Goldstone, California, USA. The city of Los Angeles is located about 200 km away in the southwest direction from Goldstone, on the other side of the mountains. Figure 2(b) presents propagation loss on the two-dimensional map within a 300-km radius of the 70-m antenna. The areas colored blue correspond to regions within the Mojave Desert that are not separated from Goldstone by a mountain barrier. Figure 2(c) presents the horizon elevation angles as seen by the 70-m antenna. The lower horizon elevation angles in the east and west directions further reduce the propagation losses from these directions.

Example 2: Canberra, Australia. Figure 3(a) presents the terrain elevation profile and the propagation-loss values along a radial direction at an azimuth angle of 45 deg from the 70-m antenna site (DSS 43) at Tidbinbilla. The city of Canberra is about 20 km away along this direction. Figure 3(B) presents propagation loss on the two-dimensional map within a 300-km radius of the 70-m antenna. The areas in the north to northwest and in the south of DSS 43 have lower propagation losses, as a result of lower horizon elevation angles along these directions. Figure 3(c) presents the horizon elevation angles as seen by the 70-m antenna.

Example 3: Robledo, Spain. Figure 4(a) presents the terrain elevation profile and the propagation-loss values along a radial direction at an azimuth angle of 90 deg from the 70-m antenna site (DSS 63) at Robledo. Madrid City is about 50 km away in this direction without large mountains in between. Figure 4(b) presents propagation loss on the two-dimensional map within a 300-km radius of the 70-m antenna. A large area of low propagation loss is clearly visible in the south, as the horizon elevation angle of DSS 63 is low in the south. Figure 4(c) presents the horizon elevation angles as seen by the 70-m antenna.

VI. Conclusion

This article presents a method for predicting losses in trans-horizon propagation from sources distributed in an area to an Earth station beyond a line of sight. The area can be any specific area of interest or the entire region surrounding the Earth station. The method takes into account detailed terrain data of the region and makes predictions using the atmosphere-dependent propagation models recommended by the ITU. The result is a map of propagation losses for the region at a given frequency and time percentile. The numerical databases of the calculated losses allow prediction of area-to-point trans-horizon interferences. The color-coded propagation-loss map provides a visible overview of the region centered at the Earth station, indicating for every geographic area the effective radio-frequency isolation from the Earth station as provided by the terrain. To protect the deep-space Earth stations from harmful interference, restrictions will be needed on the future deployment of high-density commercial services in areas with insufficient terrain isolation.

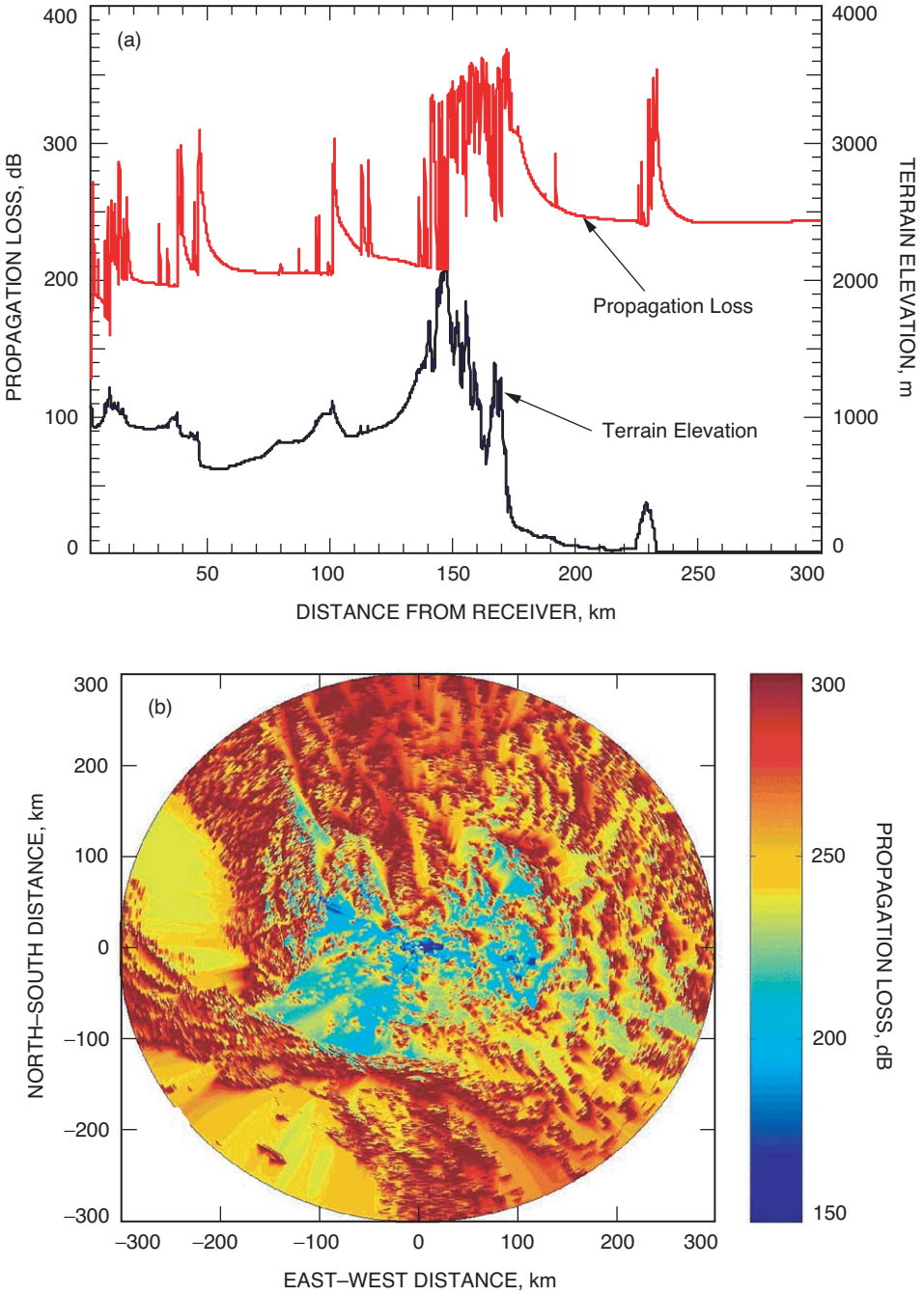

Fig. 2. Goldstone, California, USA: (a) propagation loss and terrain along azimuth angle 217 deg of DSS 14, loss calculated at 32 GHz, exceeded all but 0.001 percent of the time; (b) propagation losses within 300 km of DSS 14, loss calculated at 32 GHz, exceeded all but 0.001 percent of the time, in decibels; and (c) horizon elevation angles as seen by DSS 14.

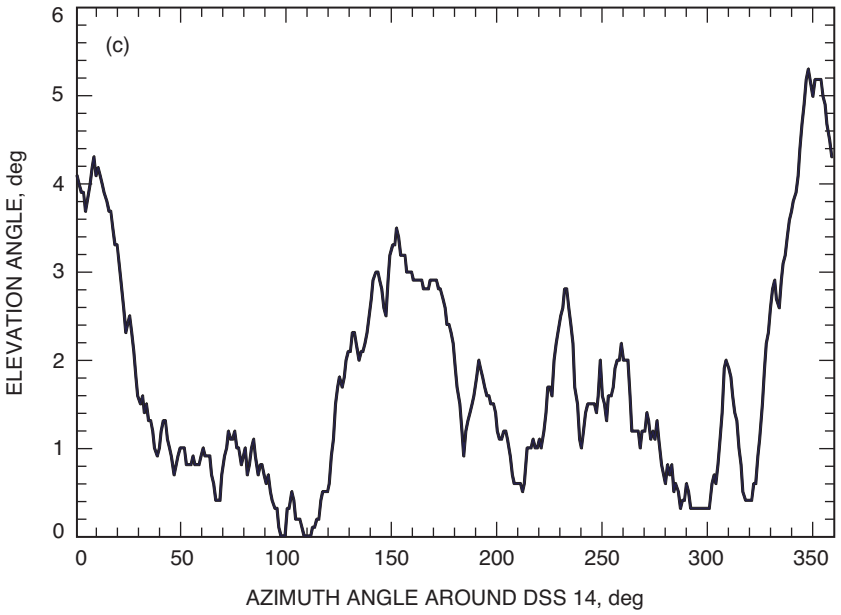

Fig. 2 (cont'd.).

Acknowledgments

We appreciate Paul McKenna and Greg Hand from the NTIA Institute for Telecommunication Sciences (ITS) for providing the global high-resolution terrain data and Telecommunications Analysis (TA) services. We are also indebted to Charles Lee for his help in making a MATLAB code for extracting terrain data files. Kelly Gritton is credited for developing the mapping software at an initial phase of this study. We would like to thank Boonsieng Benjauthrit and Anil Kantak for reviewing this article and providing many valuable comments on the article.

References

[1] International Telecommunication Union, "International Mobile Telecommunications-2000 (IMT-2000)," Recommendation ITU-R M.687, 1997.

[2] C. M. Ho, M. K. Sue, T. K. Peng, and E. K. Smith, "Terrestrial Propagation of 2-Gigahertz Emissions Transmitted from the Deep Space Network 70-Meter Antenna at Robledo," *The Interplanetary Network Progress Report 42-152, October–December 2002*, Jet Propulsion Laboratory, Pasadena, California, pp. 1–22, February 15, 2003.
http://ipnpr.jpl.nasa.gov/progress_report/42-152/152C.pdf

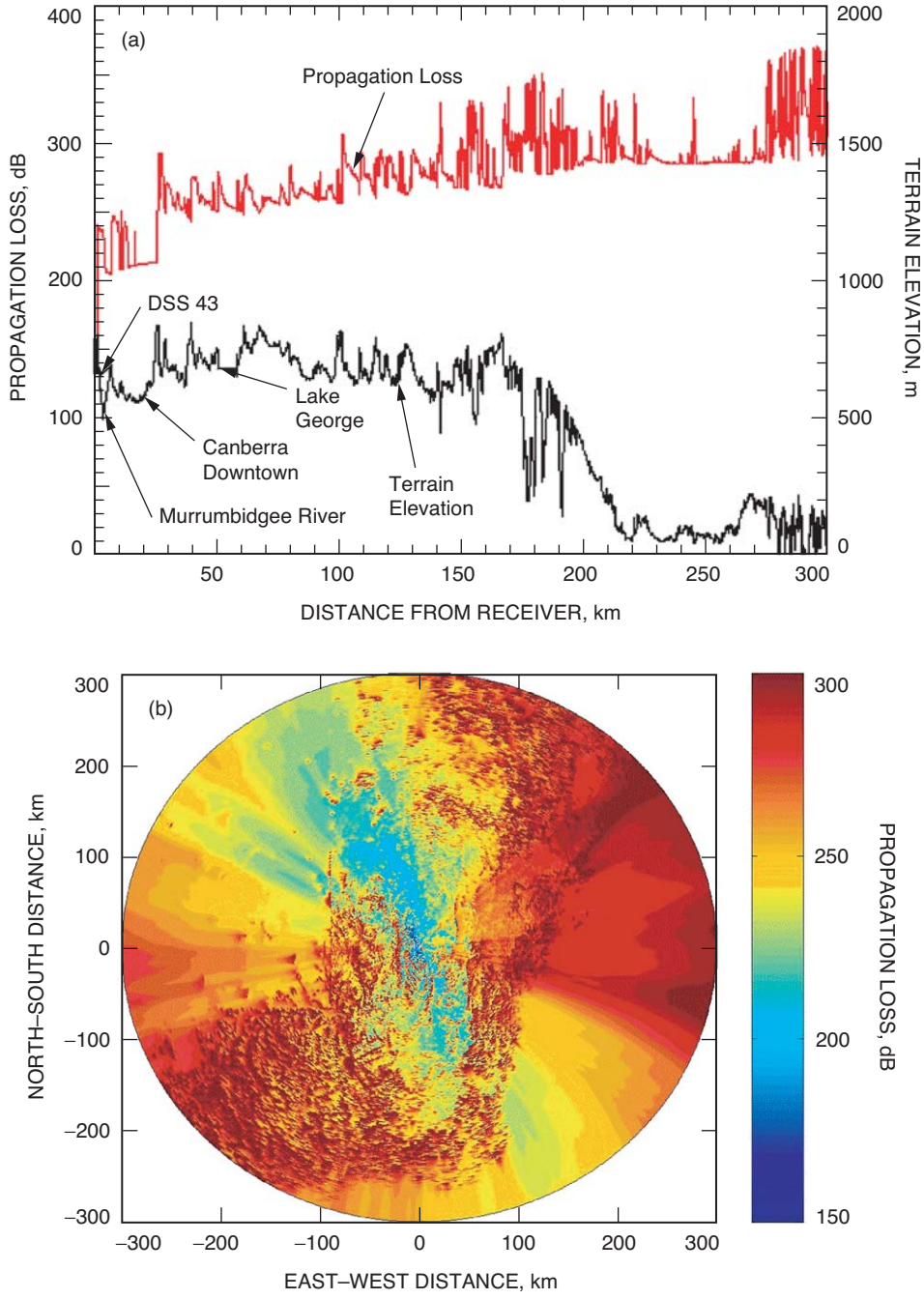

Fig. 3. Canberra, Australia: (a) propagation losses and terrain along azimuth angle 45 deg of DSS 43, loss calculated at 32 GHz, exceeded all but 0.001 percent of the time; (b) propagation losses within 300 km of DSS 43, loss calculated at 32 GHz, exceeded all but 0.001 percent of the time, in decibels; and (c) horizon elevation angles as seen by DSS 43.

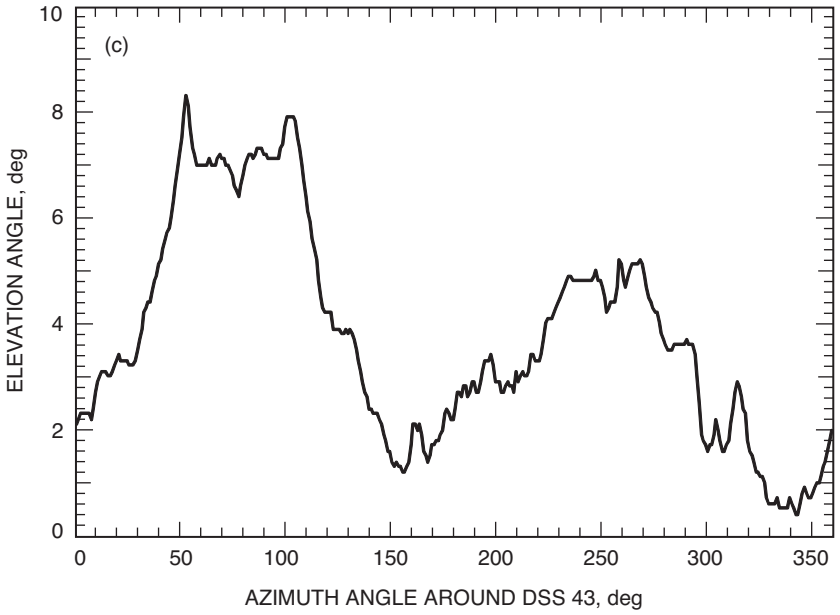

Fig. 3 (cont'd.).

[3] C. Ho, M. Sue, and C. Ruggier, "An Estimate of Interference Effect From the Los Angeles Area High-Density Fixed Services (HDFS) on the Goldstone DSN Receiver Above 30 GHz: Monte Carlo Simulation," *The Telecommunications and Mission Operations Progress Report 42-138, April–June 1999*, Jet Propulsion Laboratory, Pasadena, California, pp. 1–18, August 15, 1999. http://ipnpr.jpl.nasa.gov/progress_report/42-138/138C.pdf

[4] *DSMS Telecommunications Link Design Handbook*, 810-005, Jet Propulsion Laboratory, Pasadena, California, May 5, 2005.

[5] International Telecommunication Union, "Protection Criteria for Deep-Space Research," Recommendation ITU-R SA.1157, 1995.

[6] International Telecommunication Union, "Protection Criteria for the Space Research Service in the 37-38 GHz and 40-40.5 GHz Bands," Recommendation ITU-R SA.1396, 1999.

[7] International Telecommunication Union, "Radio Regulations," Appendix 7, ITU-R, Geneva, 2001.

[8] L. J. Ippolito, *Propagation Effects Handbook for Satellite Systems Design, A Summary of Propagation Impairments to 10 to 100 GHz Satellite Links With Techniques for System Design*, NASA Reference Publication 1082(04), 1989.

[9] R. K. Crane, "A Review of Transhorizon Propagation Phenomena," *Radio Science*, vol. 16, no. 5, pp. 649–669, 1981.

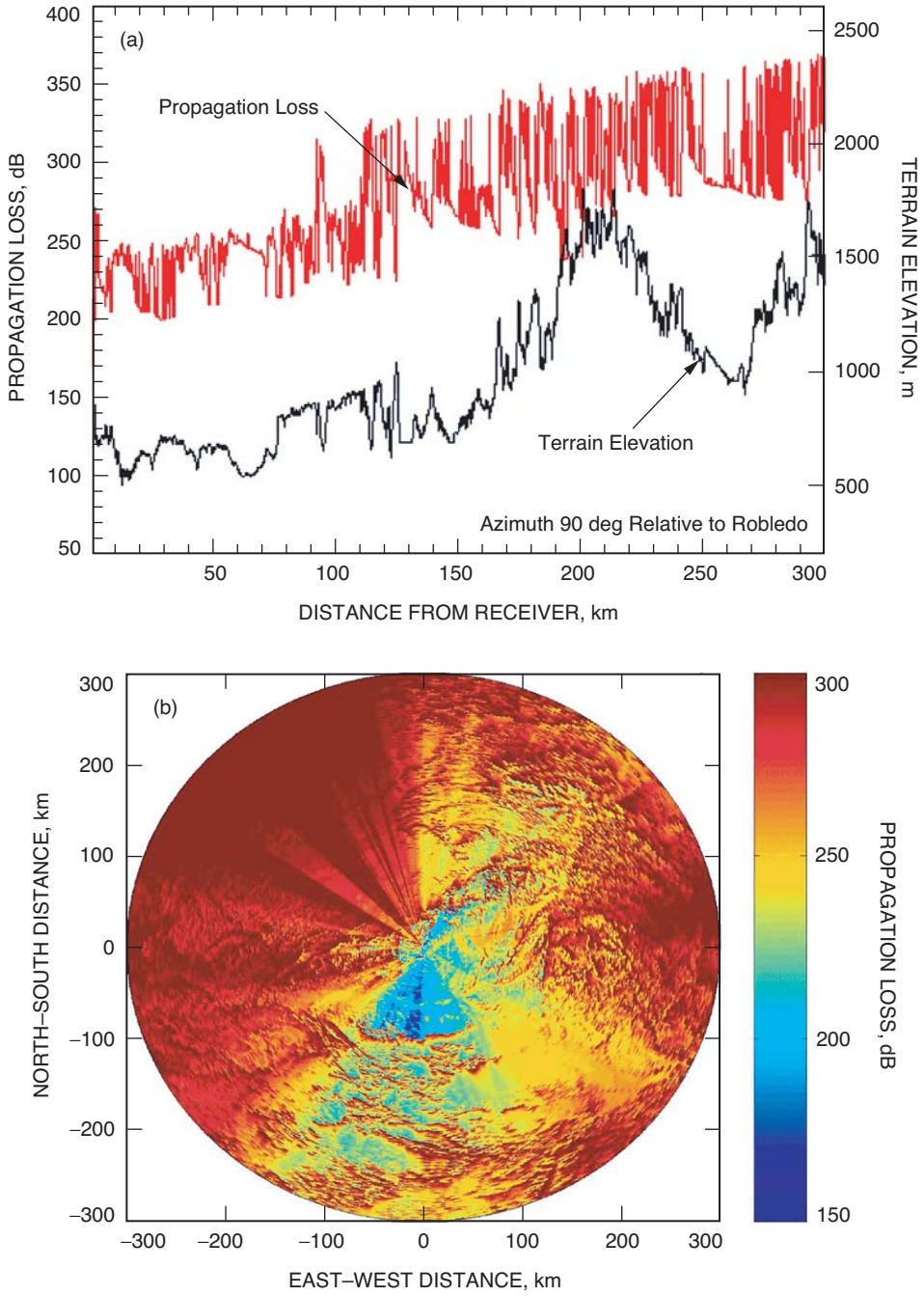

Fig. 4. Robledo, Spain: (a) propagation loss and terrain along azimuth angle 90 deg of DSS 63, loss calculated at 32 GHz, exceeded all but 0.001 percent of the time; (b) propagation losses within 300 km of DSS 63, loss calculated at 32 GHz, exceeded all but 0.001 percent of the time, in decibels; and (c) horizon elevation angles as seen by DSS 63.

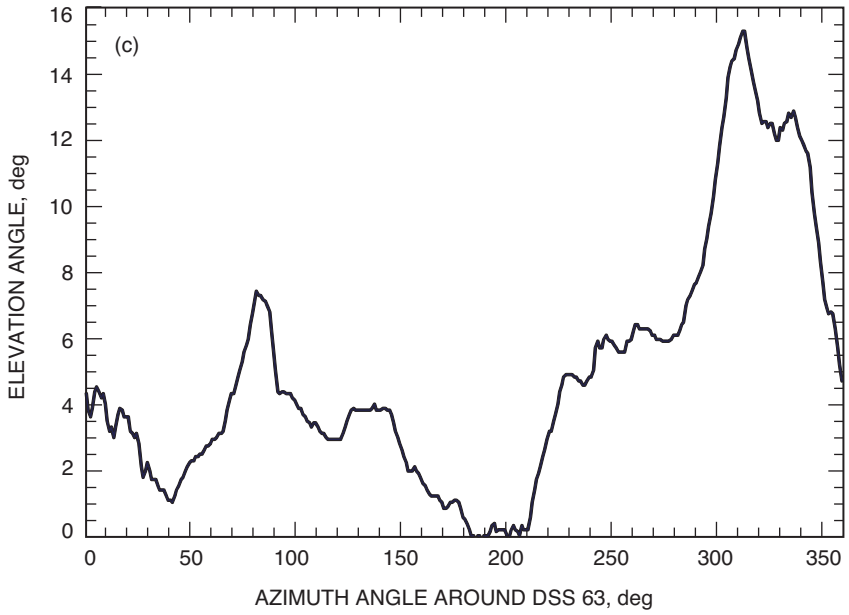

Fig. 4. (cont'd).

[10] International Telecommunication Union, "Prediction Procedure for the Evaluation of Microwave Interference Between Stations on the Surface of the Earth at Frequencies above about 0.7 GHz," Recommendation ITU-R P.452-10, 2001.

[11] International Telecommunication Union, "Propagation by Diffraction," Recommendation ITU-R P.526-8, 2003.

Appendix

Clear-Air Propagation-Loss Calculation Methodology

The equations used to calculate the clear-air—mode (1)—propagation losses are based on ITU-R Recommendation P.452-10 (Version 10). A Version 11 (P.452-11), containing a modified ducting/layer reflection model, also has been published, but it is in the process of being revised and so has not been relied upon here. The equations used here are somewhat simplified from those appearing in ITU-R P.452-10 [10]. The entire path from transmitter to receiver is assumed to lie over dry land. The time percentage p is assumed to be very small. (In particular, p is smaller than the time percentage for which refractive index lapse rates exceeding 100 N-units/km can be expected in the first 100 m of the lower atmosphere.) There is assumed to be no clutter. The equations used in this article for diffraction, tropospheric scatter, and ducting/layer reflection loss are summarized here.

I. Total Gaseous Absorption

The total gaseous absorption is

$$A_g = \left[\gamma_0 + \gamma_w(\rho)\right] d \text{ dB} \tag{A-1}$$

where γ_0 is the specific attenuation due to dry air; $\gamma_w(\rho)$ is the specific attenuation due to water vapor, which is a function of the water-vapor density ρ in g/m^3; and d is the great-circle path distance in kilometers. The specific attenuations are modeled as

$$\gamma_0 = \left(7.19 \times 10^{-3} + \frac{6.09}{f^2 + 0.227} + \frac{4.81}{(f-57)^2 + 1.50}\right) f^2 \times 10^{-3} \text{ dB/km} \tag{A-2}$$

$$\gamma_w(\rho) = \left(0.050 + 0.0021\rho + \frac{3.6}{(f-22.2)^2 + 8.5}\right) f^2 \rho \times 10^{-4} \text{ dB/km} \tag{A-3}$$

where f is the frequency in gigahertz.

II. Line-of-Sight Loss

When there is a direct line of sight between transmitter and receiver, the loss is

$$L_{b0}(p) = 92.5 + 20 \log f + 20 \log d + E_s(p) + A_g \text{ dB} \tag{A-4}$$

where f is the frequency in gigahertz, d is the great-circle path distance in kilometers, and p is the time percentage for which the actual loss is smaller than the calculated loss. The term $E_s(p)$ is a correction for multipath and focusing effects,

$$E_s(p) = 2.6 \left(1 - e^{-d/10}\right) \log\left(\frac{p}{50}\right) \text{ dB} \tag{A-5}$$

A_g is the total gaseous absorption as calculated from Eq. (A-1) using a water-vapor density ρ of 7.5 g/m^3.

III. Diffraction Loss

An approximate calculation of diffraction loss is based on modeling the terrain as a sequence of (at most) three knife edges. The principal edge is labeled P. The secondary edge that lies between the transmitter and the principal edge is labeled A. The secondary edge that lies between the receiver and the principal edge is labeled B. A geometric parameter is associated with each edge: v_P with P, v_A with A, and v_B with B. These geometric parameters are defined as

$$v_P = \left[h_P + \frac{d_{PT} d_{PR}}{2r_e} - \frac{h_{ts} d_{PR} + h_{rs} d_{PT}}{d}\right] \cdot \sqrt{\frac{2d}{\lambda d_{PT} d_{PR}}} \tag{A-6}$$

$$v_A = \left[h_A + \frac{d_{AT} d_{AP}}{2r_e} - \frac{h_{ts} d_{AP} + h_P d_{AT}}{d_{PT}}\right] \cdot \sqrt{\frac{2d_{PT}}{\lambda d_{AT} d_{AP}}} \tag{A-7}$$

$$v_B = \left[h_B + \frac{d_{BR} d_{BP}}{2r_e} - \frac{h_{rs} d_{BP} + h_P d_{BR}}{d_{PR}}\right] \cdot \sqrt{\frac{2d_{PR}}{\lambda d_{BR} d_{BP}}} \tag{A-8}$$

In these equations, h_P, h_A, and h_B are the heights of the three edges above mean sea level, and h_{ts} and h_{rs} are the center heights of the transmitting and receiving antennas above mean sea level. The distances are defined as follows: d is the total path length from transmitter to receiver, d_{PT} is the distance separating the principal edge from the transmitter, d_{PR} is the distance separating the principal edge from the receiver, d_{AT} is the distance separating the secondary edge A from the transmitter, d_{AP} is the distance between the secondary edge A and the primary edge, d_{BR} is the distance separating the secondary edge B from the receiver, and d_{BP} is the distance between the secondary edge B and the principal edge. The wavelength is λ, and r_e is the effective Earth radius, defined by

$$r_e = 3 \cdot 6371 = 19,113 \text{ km} \tag{A-9}$$

The diffraction loss, as a positive decibel quantity, is calculated by

$$L_{bd}(p) = 92.5 + 20 \log f + 20 \log d + L_d(p) + E_{sd}(p) + A_g \text{ dB} \tag{A-10}$$

where f is the frequency in gigahertz, d is the great-circle path distance in kilometers, and p is the time percentage for which the actual loss is smaller than the calculated loss. The term $E_{sd}(p)$ is a correction for multipath effects between the antennas and the horizon obstacles,

$$E_{sd}(p) = 2.6 \left(1 - e^{-(d_{Lt}+d_{Lr})/10}\right) \log\left(\frac{p}{50}\right) \text{ dB} \tag{A-11}$$

when $d_{Lt} + d_{Lr} \leq d$. Otherwise, $d_{Lt} + d_{Lr}$ is replaced by d in Eq. (A-11). The sea-level arc distances, in kilometers, to the radio horizon obstacle from the transmitting and receiving antennas are d_{Lt} and d_{Lr}, respectively, and A_g is the total gaseous absorption as calculated from Eq. (A-1) using a water-vapor density ρ of 7.5 g/m^3.

The excess diffraction loss $L_d(p)$ is, for small p, calculated as

$$L_d(p) = J(\nu_P) + T\big[J(\nu_A) + J(\nu_B) + C\big] \text{ dB} \tag{A-12}$$

where

$$C = 10.0 + 0.04 \text{ dB} \tag{A-13}$$

$$T = 1.0 - \exp\left[\frac{-J(\nu_P)}{6.0}\right] \tag{A-14}$$

$$J(\nu) = 6.9 + 20 \log\left(\sqrt{(\nu - 0.1)^2 + 1} + \nu - 0.1\right) \text{ dB} \quad (\nu > -0.78) \tag{A-15}$$

and the geometric parameters are calculated from Eqs. (A-6) through (A-8). If $\nu_P \leq -0.78$, $L_d(p) = 0$ dB.

IV. Tropospheric Scatter Loss

The tropospheric scatter loss has a strong dependence on the angular path distance θ, which is defined as

$$\theta = \frac{d}{a_e(50\%)} + \theta_{et} + \theta_{er} \tag{A-16}$$

The $a_e(50\%)$ is the mean effective radius of the Earth, taking refraction in the atmosphere into account; it is given by

$$a_e(50\%) = 6371 \cdot \frac{157}{157 - \Delta N_{50}} \tag{A-17}$$

where ΔN_{50} is the average radio-refractive index lapse rate through the lowest 1 km of the atmosphere. In the calculations reported here, $\Delta N_{50} = 45$, and $a_e(50\%) = 8931$ km. The angular path distance depends on the horizon elevation angle as seen from the transmitter,

$$\theta_{et} = \frac{h_{Lt} - h_{ts}}{d_{Lt}} - \frac{d_{Lt}}{2a_e(50\%)} \tag{A-18}$$

and on the horizon elevation angle as seen from the receiver,

$$\theta_{er} = \frac{h_{Lr} - h_{rs}}{d_{Lr}} - \frac{d_{Lr}}{2a_e(50\%)} \tag{A-19}$$

In these equations, h_{Lt} and h_{Lr} are the heights of the horizon obstacles above mean sea level as seen from the transmitter and receiver, respectively.

The tropospheric scatter loss, as a positive decibel quantity, is calculated by

$$L_{bs}(p) = 190 + L_f + 20\log d + 0.573\,\theta - 0.15N_0 + L_c + A_g - 10.1\left[-\log\left(\frac{p}{50}\right)\right]^{0.7} \text{ dB} \tag{A-20}$$

where d is the great-circle path distance in kilometers, θ is the path angular distance in milliradians, N_0 is the sea-level surface refractivity, and p is the time percentage for which the actual loss is smaller than the calculated loss. The frequency-dependent loss L_f is given by

$$L_f = 25\log f - 2.5\left[\log\left(\frac{f}{2}\right)\right]^2 \text{ dB} \tag{A-21}$$

where f is the frequency in gigahertz. A_g is the total gaseous absorption as calculated from Eq. (A-1) using a water-vapor density ρ of 3 g/m^3. The aperture-to-medium coupling loss L_c is a function of transmit and receive antenna gains (G_t and G_r, both in dBi) in the direction of the scatter volume,

$$L_c = 0.051 \cdot e^{0.055(G_t + G_r)} \text{ dB} \tag{A-22}$$

The loss term L_c is typically very small. The boresights of the transmit and receive antennas do not ordinarily point in the direction of the scatter volume, so the sum $G_t + G_r$ is typically not large. For $G_t + G_r = 50$ dB, $L_c = 0.8$ dB. Typically, $G_t + G_r \ll 50$ dB, so L_c is typically less than one decibel.

V. Ducting/Layer Reflection Loss

The first step in modeling the ducting/layer reflection loss is to create a least-squares, straight-line fit for terrain height as a function of distance. Then, for each location of interest, there are two heights: the actual terrain height and the straight-line-fit height. Both of these heights are measured relative to the mean sea level. From this geometrical modeling come three essential parameters: h_{st} is the minimum of the straight-line-fit height and the actual terrain height at the transmitter location; h_{sr} is the minimum of the straight-line-fit height and the actual terrain height at the receiver location; and, finally, the terrain roughness, denoted h_m, is defined as the maximum value (over all possible locations along the path from the transmitter to the receiver) of the difference between the actual terrain height and the straight-line-fit height for the same location. The height parameters h_{te} and h_{re} are defined by

$$h_{te} = h_{ts} - h_{st} \tag{A-23}$$

$$h_{re} = h_{rs} - h_{sr} \tag{A-24}$$

where h_{ts} and h_{rs} are the center heights of the transmitting and receiving antennas above mean sea level.

The anomalous (ducting/layer reflection) loss, as a positive decibel quantity, is calculated from

$$L_{ba}(p) = A_f + A_d(p) + A_g \text{ dB} \tag{A-25}$$

The total gaseous absorption A_g is calculated from Eq. (A-1) using a water-vapor density ρ of 7.5 g/m^3.

The total fixed coupling loss A_f is given by

$$A_f = 102.45 + 20\log f + 20\log\left(d_{Lt} + d_{Lr}\right) + A_{st} + A_{sr} \text{ dB} \tag{A-26}$$

where f is the frequency in gigahertz, d_{Lt} is the horizon distance in kilometers as seen from the transmitter, and d_{Lr} is the horizon distance in kilometers as seen from the receiver.

The site-shielding diffraction losses A_{st} and A_{sr} are given by

$$A_{st} = \begin{cases} 20\log\left[1 + 0.361\,\theta_t''\sqrt{f \cdot d_{Lt}}\right] + 0.264\,\theta_t'' f^{1/3}\,\text{dB}, & \theta_t'' > 0 \\ 0\,\text{dB}, & \theta_t'' \le 0 \end{cases} \tag{A-27}$$

$$A_{sr} = \begin{cases} 20\log\left[1 + 0.361\,\theta_r''\sqrt{f \cdot d_{Lr}}\right] + 0.264\,\theta_r'' f^{1/3}\,\text{dB}, & \theta_r'' > 0 \\ 0\,\text{dB}, & \theta_r'' \le 0 \end{cases} \tag{A-28}$$

where

$$\theta_t'' = \theta_{et} - 0.1\,d_{Lt} \text{ mrad} \tag{A-29}$$

$$\theta_r'' = \theta_{er} - 0.1\,d_{Lr} \text{ mrad} \tag{A-30}$$

The horizon elevation angles θ_{et} and θ_{er} are given by Eqs. (A-18) and (A-19).

The time percentage and angular distance dependent losses $A_d(p)$ are given by

$$A_d(p) = \gamma_d \cdot \theta' + A(p) \text{ dB} \tag{A-31}$$

where the specific attenuation γ_d is

$$\gamma_d = 5 \times 10^{-5}\, a_e(50\%)\, f^{1/3} \text{ dB/mrad} \tag{A-32}$$

In Eq. (A-31), the corrected angular distance θ' is defined by

$$\theta' = \frac{10^3 d}{a_e(50\%)} + \theta'_t + \theta'_r \text{ mrad} \tag{A-33}$$

where d, the great-circle path distance, is in units of kilometers and

$$\theta'_t = \min(\theta_{et}, 0.1\, d_{Lt}) \text{ mrad} \tag{A-34}$$

$$\theta'_r = \min(\theta_{er}, 0.1\, d_{Lr}) \text{ mrad} \tag{A-35}$$

and $a_e(50\%)$ is given by Eq. (A-17).

The time percentage variability $A(p)$ is given by

$$A(p) = -12 + (1.2 + 3.7 \times 10^{-3} d) \log\left(\frac{p}{\beta}\right) + 12 \left(\frac{p}{\beta}\right)^{\Gamma} \text{ dB} \tag{A-36}$$

where

$$\Gamma = \frac{1.076}{(2.0058 - \log\beta)^{1.012}} \times e^{-(9.51 - 4.8 \log\beta + 0.198(\log\beta)^2) \times 10^{-6} \cdot d^{1.13}} \tag{A-37}$$

and

$$\beta = \beta_0 \cdot \mu_2 \cdot \mu_3 \tag{A-38}$$

The parameter β represents a percentage and is constrained by $\beta \leq 100$. The parameter β_0 is given by

$$\beta_0 = 10^{-0.015|\varphi| + 1.67} \mu_1\, \mu_4 \tag{A-39}$$

where φ is the path center latitude in degrees. The parameter μ_1 is given by

$$\mu_1 = \left(10^{-d/16 - 6.6\tau} + \left[10^{-(0.496 + 0.354\tau)}\right]^5\right)^{0.2} \tag{A-40}$$

but μ_1 is limited to being less than or equal to 1. The parameter μ_4 is given by

$$\mu_4 = 10^{(-0.935+0.0176|\varphi|)\log\mu_1} \tag{A-41}$$

The parameter τ is

$$\tau = 1 - e^{-(4.12\times10^{-4}\times d^{2.41})} \tag{A-42}$$

In Eq. (A-38), the parameter μ_2 is given by

$$\mu_2 = \left(\frac{500}{a_e(50\%)}\frac{d^2}{\left(\sqrt{h_{te}}+\sqrt{h_{re}}\right)^2}\right)^{\alpha} \tag{A-43}$$

where h_{te} and h_{re} are given in Eqs. (A-23) and (A-24), and where α is given by

$$\alpha = -0.6 - 3.5\times10^{-9}\cdot d^{3.1}\cdot\tau \tag{A-44}$$

In Eq. (A-38), the parameter μ_3 is assigned the value 1 if the terrain roughness is $h_m \le 10$ m. Otherwise (usually), μ_3 is calculated from

$$\mu_3 = \exp\left(-4.6\times10^{-5}(h_m-10)(43+6d_{\text{int}})\right) \tag{A-45}$$

where

$$d_{\text{int}} = \min(d - d_{Lt} - d_{Lr}, 40)\ \text{km} \tag{A-46}$$

VI. Overall Prediction of Trans-Horizon Loss

For a specific transmitter location and a specific receiver location, the loss of each of the above three clear-air propagation mechanisms is calculated and compared to the others. It is commonly the case that the propagation loss of one dominant mechanism is well less than that of either of the other two mechanisms. In such a case, the trans-horizon loss may be approximated as the propagation loss of this dominant mechanism.

In general, however, it is necessary to have a formula to combine the diffraction, tropospheric scatter, and ducting/layer reflection losses. Here is the formula that is recommended in ITU-R P.452-10, Table 5 [10], for overall prediction and is used to compute the results in this article:

$$L_b(p) = -5\log\left(10^{-0.2L_{bs}(p)} + 10^{-0.2L_{bd}(p)} + 10^{-0.2L_{ba}(p)}\right)\ \text{dB} \tag{A-47}$$

where $L_b(p)$ is the trans-horizon loss in positive decibels. This scheme combines the component losses by first converting the positive-decibel component losses to fractional, dimensionless losses; then computing a root-sum-square; and then converting the combined (fractional, dimensionless) loss into positive decibels. If one component loss dominates (that is, if the positive-decibel loss of one component is well less than that of either of the other components), then the combining scheme of Eq. (A-47) produces a trans-horizon loss nearly equal to the dominant component loss. If two or more component losses are near in value,

then the combining scheme of Eq. (A-47) produces a trans-horizon loss that is somewhat less than the smallest component loss. In other words, the received interference power that is computed by using the combining scheme of Eq. (A-47) is somewhat more than that due to any single propagation mechanism.

For short distances, the loss given by the ducting loss model of ITU-R P.452-10 can be less than the line-of-sight loss, causing the overall prediction also to be less than the line-of-sight loss. In these cases, the line-of-sight loss $L_{b0}(p)$ from Eq. (A-4) is substituted for the combined loss of Eq. (A-47).